



Voltammetric investigations on the relative deactivation of boron-doped diamond, glassy carbon and platinum electrodes during the anodic oxidation of substituted phenols in room temperature ionic liquids

KR. Saravanan, S. Sathyamoorthi, D. Velayutham, V. Suryanarayanan*

CSIR-Central Electrochemical Research Institute, Karaikudi, 630 006 India

ARTICLE INFO

Article history:

Received 5 December 2011
Received in revised form 21 February 2012
Accepted 21 February 2012
Available online 1 March 2012

Keywords:

Boron-doped diamond
Glassy carbon
Cyclic voltammetry
Phenols
Room temperature ionic liquids

ABSTRACT

Deactivation behaviour of boron-doped diamond (BDD) had been extensively studied for the first time in three room temperature ionic liquids (RTILs) namely 1-ethyl-3-methyl imidazolium nonaflate (EMIN), triethylmethylammonium methyl sulphate (TEMAMS) and N-hexyl-N,N,N-triethylammonium bis(trifluoromethanesulfonyl)imide (N_{2226} TFSI) along with glassy carbon (GC) and platinum (Pt) electrodes on the anodic oxidation of 2,6-dimethylphenol (2,6-DMP), 2,4-dimethylphenol (2,4-DMP) and 3,4-methylenedioxyphenol (3,4-MDP) using cyclic voltammetry (CV). Voltammetric studies reveal that the anodic potential limit of the electrodes decreases in the order $GC > BDD > Pt$ in these media and EMIN shows the highest anodic limit among the three RTILs. Multisweep CV studies suggest that the three phenols show irreversible and reversible characteristics on the BDD and Pt electrodes respectively. On the other hand, they exhibit reversible redox behaviour in TEMAMS and irreversible nature in EMIN and N_{2226} TFSI media on the GC electrode. The phenolic compounds get oxidised at higher potential on the BDD electrode followed by Pt and GC electrodes and their oxidation potential in the three media increases in the order: TEMAMS < EMIN < N_{2226} TFSI. Anodic polarisation studies in presence of phenols suggests that the Pt and GC do not show any serious electrode fouling; however, the BDD gets deactivated severely, as noted from the J_{pa}^4/J_{pa}^1 values. Passivation of the BDD electrode in the EMIN medium containing the 2,6-DMP was investigated by Scanning Electron Microscopy (SEM) and Atomic Force Microscopy (AFM). The effect of acetonitrile (CH_3CN) on the activation of the BDD electrode surface was also studied in detail.

© 2012 Elsevier Ltd. All rights reserved.

1. Introduction

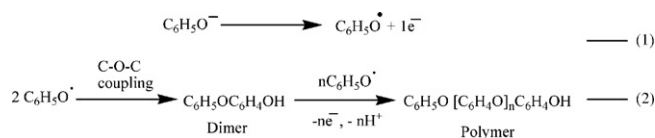
Phenols and related compounds have high toxicity as well as low water solubility and are persistent pollutants of the environment [1,2]. They are potentially fatal if ingested, inhaled and absorbed by skin and may cause severe burns and affect central nervous system, liver and kidney. Electrochemical methods are of prime importance for detecting various phenolic compounds and their treatment [3–6].

During the detection and the anodic oxidation of phenolic compounds in the aqueous media, formation of polymeric film on the electrode surface represents a serious problem because they cause rapid deactivation of electrode by blocking electron transfer and slowing down further oxidation. Studies are available in the literature about the electropolymerisation of phenols on various

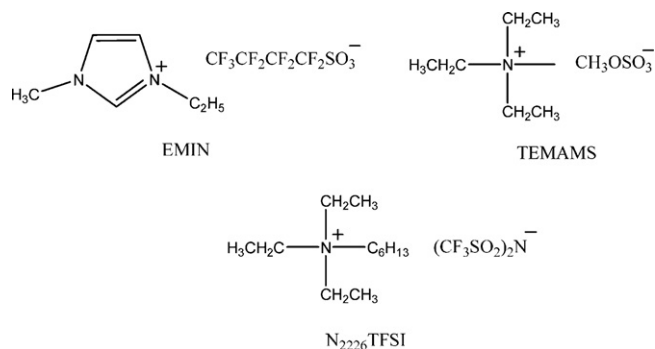
electrodes such as Au [7], glassy carbon [8], Pt [9–13], PbO_2 [14,15] etc. The globally accepted mechanism for the electropolymerisation in the aqueous medium is the generation of phenoxy radical by one electron oxidation of phenolate anion, followed by the reaction of the former with another radical or with an unreacted phenolate anion monomer to form dimeric products and then polymers (Scheme 1). The oligomers and polymers formed during the course of oxidative process can naturally adsorb on any electrode surface and passivate it. Choosing appropriate electrode material and medium may be an alternative strategy for carrying out the electrooxidation reaction successfully.

One such green medium is ionic liquid, which attracts considerable attention during the past few years. Ionic liquids are environmentally safe due to absence of any vapour pressure and therefore promise to make synthetic processes more efficient [16–18]. From the electrochemical point of view, some of them have excellent properties such as wide potential window and high conductivity [19–21]. They have been used as electrolytes in the basic studies on the electrochemistry of organic compounds [22,23]. The potential of the ionic liquids as the media for the electro synthesis

* Corresponding author. Tel.: +91 4565 227772; fax: +91 4565 227779.
E-mail addresses: vidhyasur@yahoo.co.in, surya@cecri.res.in
(V. Suryanarayanan).



Scheme 1. Reaction mechanism of electro polymerisation of phenol.



Scheme 2. Chemical structure of the synthesised RTILs.

of conducting polymers such as polyaniline (PANi), poly(3,4-ethylenedioxythiophene) (PEDOT), polyphenylene and polypyrrole was successfully demonstrated [24–27].

Electrode material plays an important role in suppressing the fouling during electrochemical reactions. Among different electrode materials studied so far, boron-doped diamond (BDD) electrode is distinguished from conventional electrodes because of several important technological properties such as extremely wide potential window, corrosion stability in very aggressive media, an inert surface with low adsorption properties, a strong tendency to resist deactivation and robust oxidation capacity [28,29]. Synthetic utility of the BDD anode had been extensively studied on the electrooxidation of phenol, 3-methylpyridine and salicylic acid in aqueous media [30–32].

In recent studies, ammonium and imidazolium cations based ionic liquids had been used as the media for the oxidative coupling reaction on the BDD anode [33–35]. Hence, the possibility on the combined use of ionic liquid as the medium and the BDD as the anode seems to be an attractive protocol for carrying out the anodic oxidation of organic compounds without electrode fouling. Until now, no work is attempted to investigate the fundamental aspects on the electrochemistry of BDD electrode in ionic liquid medium containing phenols.

With such a background, for the first time, the electrochemical behaviour of the BDD has been studied along with glassy carbon (GC) and Pt electrodes on the electrooxidation of 2,4-dimethyl phenol (2,4-DMP), 2,6-dimethyl phenol (2,6-DMP) and 3,4-methylenedioxyphenol (3,4-MDP) in three RTILs. The chemical structure of 1-ethyl-3-methyl imidazolium nonaflate (EMIN), triethylmethylammonium methyl sulphate (TEMAMS) and N-hexyl-N,N,N-triethylammonium bis(trifluoromethanesulfonyl)imide (N₂₂₂₆TFSI) are shown Scheme 2. The anode materials have been chosen in order to study about the influence of sp³ (BDD) and sp² (GC) and polycrystalline (Pt) structural functionalities on the electrode fouling. The voltammetric characteristics such as anodic peak potential (*E*_{pa}), anodic peak current (*I*_{pa}) and multisweep cyclic voltammetric responses were explored on the anodic oxidation of three phenols in the three media with the three electrodes.

2. Experimental

Substituted phenols such as 2,4-DMP, 2,6-DMP and 3,4-MDP were purchased from Alfa Aesar as the highest grade available and used without any further purification.

The RTIL, triethylmethylammonium methyl sulphate (TEMAMS) had been prepared, according to the literature [34]. The fluoride based anion containing RTILs had been synthesised by metathesis reaction: N-hexyl-N,N,N-triethylammonium bis(trifluoromethanesulfonyl)imide (N₂₂₂₆TFSI) was prepared using the method described in the reference [36] whilst 1-ethyl-3-methyl-imidazolium nonaflate (EMIN) was synthesised according to [37] except that 1-ethyl-3-methyl imidazolium bromide was used instead of tetrabutylammonium bromide. The synthesised RTILs were analysed using ¹H NMR spectrum for their purity and ion-chromatography for their halide content. These analyses showed that the RTILs were of comparable quality to the commercially available products.

Thin film BDD electrode (1 cm × 1 cm, exposed area is 0.2 cm²) deposited on monopolar polycrystalline silicon (Adamant Technologies, Switzerland) was used for the voltammetric and surface morphologic studies. The film thickness was approximately 0.5 mm with an average electrical resistivity of 0.75 × 10⁻³ Ω m, which corresponds to the average values obtained over set of different BDD samples with maximum variation of ±15%. The GC and Pt wire with the exposed area of 0.07 and 0.66 cm² were used as working electrodes, in addition to the BDD. A single compartment cell was used with Pt foil as counter electrode and saturated calomel electrode (SCE) as the reference electrode. The SCE was connected to the electrochemical cell through two agar-agar salt bridges where the far end of the first salt bridge and the rear end of the second one were dipped in one beaker containing the same electrolyte employed for the CV study. Prior to each voltammetric study, the rear end of the first salt bridge was washed with water followed by the electrolyte and dried in order to ensure no contamination by the chloride ions.

The BDD was activated by keeping the electrode at an anodic potential of 3.0 V vs. SCE for 5 min in aqueous acidic solution. On the other hand, the GC electrode was polished with different emery sheets starting from 1/0, 2/0, 3/0, and 4/0 (John Oakey, England), followed by washing with triple distilled water and trichloroethylene to get reproducible voltammograms. In case of Pt, the electrode was kept in concentrated nitric acid for two hours after each experiment. Then, it was cleaned with triple distilled water, dried and used as such.

The CV measurements were recorded using an Eco Chemie Autolab Potentiostat system under computer control. The morphology of the electrode surface was characterised by scanning electron microscope (SEM) with a JEOL JSM6480LV system and atomic force microscope (AFM) with Agilent Technology Inc., SPM 5500. Proton NMR spectra were recorded with 400 MHz Bruker NMR Spectrometer with CDCl₃ and TMS as solvent and internal reference respectively. Ion-Chromatographic separation was performed on Metrohm ion chromatography system (Metrohm AG, Herisau, Switzerland) consisted of the following: 818 IC pump, 837 IC eluent degasser, 830 IC interface, 820 IC Separation Center, Rheodyne injection valve, Metrodata 2.3 software, autosampler (838 Advanced Sample Processor) and conductivity detector (819 IC). All experiments were carried out at 303 ± 1 K.

3. Results and discussion

3.1. Background potential limit

The accessible anodic potential limits obtained from background voltammograms of the GC, BDD and Pt in the three RTILs

Table 1

Anodic potential limit and conductivity data of the of the synthesised RTILs on GC, Pt and BDD electrodes.

RTIL	GC (V) ^a	BDD (V) ^a	Pt (V) ^a	Conductivity (mS cm ⁻¹)	Ref.
EMIN	2.75	2.20	2.00	8.71	[37]
TEMAMS	2.55	2.14	1.94	0.83	[34]
N ₂₂₂₆ TFSI	2.19	1.94	1.80	0.67	[36]

^a Potential vs SCE.

are presented in Table 1. It is hereby noted that the potential limit is defined as range of potential observed at an anodic current density of 0.1 mA cm⁻². From Table 1, it is understandable that among the three electrodes, the GC electrode shows wide anodic potential limit in all the RTILs followed by the BDD and Pt electrodes, wherein nonaflate anion based EMIN shows the highest anodic potential limit irrespective of the nature of electrodes employed. The potential difference between the GC and BDD is higher in EMIN (almost 0.55 V) followed by TEMAMS (0.41 V) and N₂₂₂₆TFSI (almost 0.25 V). The result is found to be unusual and surprising as the previous studies on the BDD electrode in aqueous and non-aqueous solvent media reveal higher anodic potential limit for the former when compared to conventional electrodes [28].

3.2. CV studies in neat ionic liquid medium

Typical multisweep cyclic voltammograms recorded for the anodic oxidation of the 2,6-DMP (4 mM) in the TEMAMS medium on the GC, Pt and BDD electrodes at a sweep rate of 40 mV s⁻¹ are shown in Fig. 1A–C, respectively and Table 2 displays the corresponding voltammetric parameters obtained from this experiment. A reversible oxidation peak at a potential of 1.16 V and 1.47 V in the forward scan and a reduction peak at -0.05 V and -0.5 V in the reverse scan, are noted on the GC and Pt respectively (Fig. 1A and B). However, single irreversible anodic oxidation peak at a potential value of 1.60 V is noted on the BDD (Fig. 1C). The formation of reduction peak in the reverse scan on the GC and Pt may

be associated with the reduction of diphenoquinone obtained by oxidising the 2,6-DMP in the forward scan. These voltammetric results are consistent with the earlier studies carried out in 1-butyl-3-methylimidazolium tetrafluoroborate ionic liquid medium containing of 2,6-di-*t*-butyl phenol on the Pt electrode [38]. Additional redox peak noted on both the electrodes corresponds to the anodic oxidation of biphenol, produced through diphenoquinone reduction, as confirmed by the previous studies [38]. Irreversible voltammetric characteristics of the BDD in the RTILs containing phenol may be associated with the formation of electrochemically inactive intermediate/product during multisweep cycling. From the table, it is understandable that the 2,6-DMP gets oxidised at higher potential on the BDD than the GC and the Pt electrodes, however, higher peak current is noted on the GC when compared to the other electrodes at this sweep rate (Table 2).

In order to assess the effect of fouling on the electrode surface, few multisweep cyclic voltammograms (four cycles) were recorded. If the intermediates or products get irreversibly adsorbed on the electrode surface, the peak currents in the second and subsequent sweeps would be considerably low due to the formation of passive films on the electrode surface. Quantitatively, I_{pa} value obtained in the fourth cycle (I_{pa}^4) and first cycle (I_{pa}^1) is compared on each electrode and these values are presented in Table 2. From the table, it is noted that the I_{pa}^4/I_{pa}^1 values for the oxidation of the 2,6-DMP on the BDD electrode in TEMAMS medium is found to be very low, indicating severe passivation of the electrode surface. Hence, the BDD electrode was electrochemically cleaned in the aqueous acidic solution at least for 30 min. However, the I_{pa}^4/I_{pa}^1 value is found to be around 80% and 97% on the GC and Pt electrode respectively, which ensures that both electrodes do not undergo any fouling in this medium.

Next, the multisweep CVs of 2,6-DMP, 2,4-DMP and 3,4-MDP were recorded in TEMAMS, EMIN and N₂₂₂₆TFSI media on the three electrodes at a constant sweep rate of 40 mV s⁻¹ and the corresponding voltammetric parameters obtained from CVs were tabulated (Table 2). Two important voltammograms which deserve

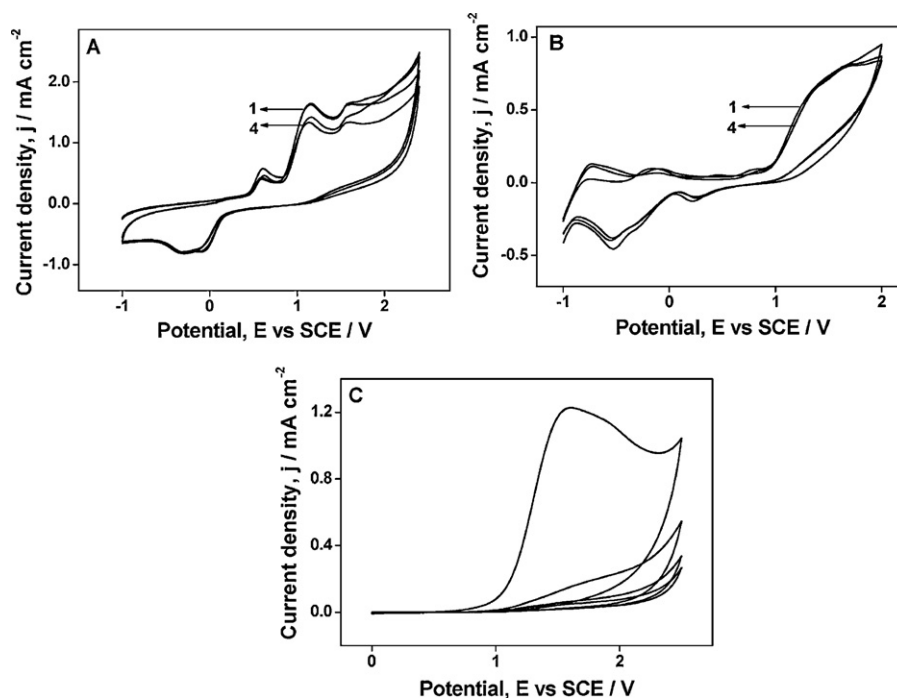


Fig. 1. Multisweep cyclic voltammograms (four cycles, 40 mV s⁻¹) on the anodic oxidation of 2,6-DMP on (A) GC, (B) Pt and (C) BDD electrodes in TEMAMS medium (concentration of the 2,6-DMP is 4 mM).

Table 2
Comparison of the voltammetric parameters obtained on the anodic oxidation of substituted phenols on the GC, Pt and BDD electrodes in the synthesised RTILs at a sweep rate 40 mV s^{-1} (concentration of phenols: $4 \times 10^{-3} \text{ mol dm}^{-3}$).

Electrode	Medium	2,6-DMP				2,4-DMP				3,4-MDP			
		E_{pa}^a (V)	I_{pa}^1 (mA cm^{-2})	I_{pa}^4 (mA cm^{-2})	I_{pa}^4/I_{pa}^1	E_{pa}^a (V)	I_{pa}^1 (mA cm^{-2})	I_{pa}^4 (mA cm^{-2})	I_{pa}^4/I_{pa}^1	E_{pa}^a (V)	I_{pa}^1 (mA cm^{-2})	I_{pa}^4 (mA cm^{-2})	I_{pa}^4/I_{pa}^1
GC	TEMAMS	1.16	1.63	1.32	0.80	1.01	1.41	0.55	0.79	0.85	2.21	1.66	0.74
	EMIN	1.58	1.16	0.88	0.76	1.27	1.00	0.80	0.80	0.98	1.77	1.70	0.96
	N_{2226} TFSI	1.65	1.30	0.90	0.70	1.50	1.20	0.85	0.71	1.17	1.10	0.86	0.78
Pt	TEMAMS	1.47	0.71	0.69	0.97	1.22	0.50	0.36	0.72	1.09	0.50	0.48	0.95
	EMIN	1.74	0.67	0.53	0.79	1.46	0.48	0.36	0.78	1.22	0.45	0.42	0.93
	N_{2226} TFSI	1.98	0.35	0.37	0.82	1.69	0.43	0.37	0.86	1.37	0.47	0.37	0.78
BDD	TEMAMS	1.60	1.22	0.28	0.23	1.73	0.52	0.12	0.26	1.93	1.32	0.56	0.42
	EMIN	1.87	0.78	0.23	0.29	1.90	0.84	0.29	0.24	1.98	0.75	0.30	0.40
	N_{2226} TFSI	2.21	0.84	0.38	0.45	2.22	0.89	0.22	0.25	2.40	1.01	0.46	0.46

^a Potential vs SCE.

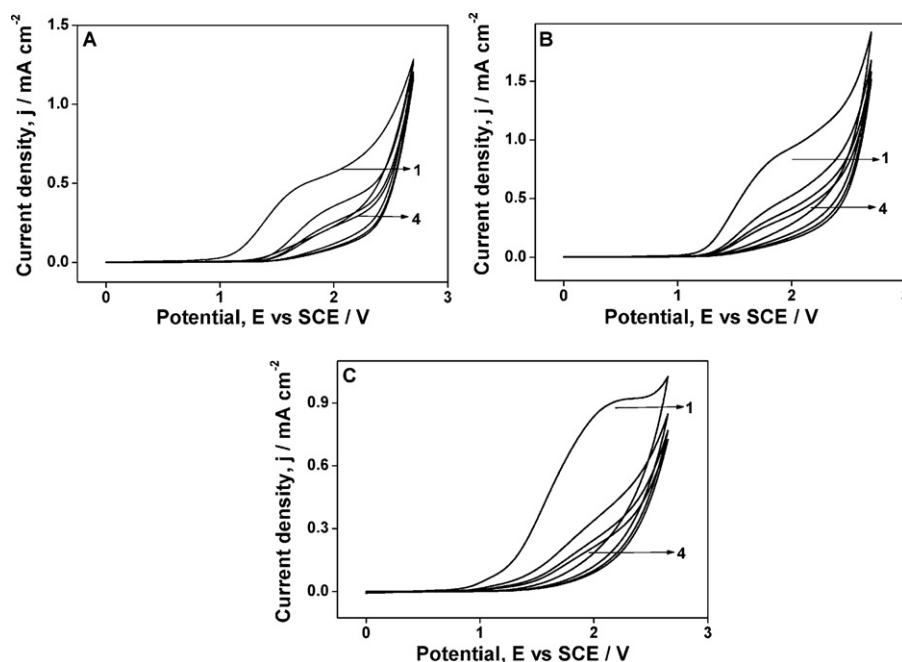


Fig. 2. Multisweep cyclic voltammograms (four cycles, 40 mV s^{-1}) of the BDD electrode on the anodic oxidation of 2,4-DMP in different media (A) TEMAMS (B) EMIN and (C) N_{2226} TFSI medium (concentration of the 2,4-DMP is 4 mM).

special characteristic features are shown here. For example, the CVs obtained for 2,4-DMP (4 mM) on the BDD in TEMAMS, EMIN, and N_{6222} TFSI media are shown in Fig. 2A–C respectively. From the figure, it is understandable that in all the three media, 2,4-DMP shows irreversible characteristic behaviour during its anodic oxidation on the BDD electrode (Fig. 2).

It is very surprising to observe that on the GC electrode, the characteristic redox behaviour noted for 2,6-DMP, 2,4-DMP and 3,4-MDP in TEMAMS changes completely into irreversible nature in the EMIN and N_{2226} TFSI media (Fig. 3). On the other hand, the above compounds show reversible and irreversible behaviour on the Pt and the BDD respectively in all the media under identical experimental conditions (Figure not shown).

The Table 2 reveals that the three phenolic compounds get oxidised at higher potential on the BDD electrode followed by Pt and GC. This is also consistent with recent works carried out in our laboratory on the comparative evaluation of the BDD and GC electrodes in different aqueous electrolyte media [39,40] and elsewhere on the anodic oxidation of ascorbic acid [41] bromide [42] and reduction of chlorine [43]. The oxidation potential of the phenols in the three

media increases in the order: TEMAMS < EMIN < N_{2226} TFSI. Among the three phenolic compounds, 2,6-DMP shows highest oxidation potential followed by 2,4-DMP and 3,4-MDP in the three media. However, on the BDD electrode, a reverse trend on the anodic peak potential is noted (Table 2).

Moreover, the phenolic compounds show highest anodic peak current density on the GC electrode followed by the BDD and Pt in three media. Particularly, in the TEMAMS medium, high anodic current density is noted on the three electrodes, which may be correlated with its lower viscosity when compared to others. Further, the average I_{pa}^4/I_{pa}^1 values obtained for the three compounds are high on both the Pt and GC electrodes. However, on the BDD electrode, the I_{pa}^4/I_{pa}^1 values for 2,6-DMP and 2,4-DMP are found to be very low and in RTILs containing 3,4-MDP, it is found to be slightly better. This reveals that the BDD electrode gets severely deactivated in all the ionic liquid media during the anodic oxidation of 2,4-DMP and 2,6-DMP.

Next, the fouled BDD electrode, obtained by anodic cycling, was characterised using scanning electron microscopy (SEM) and atomic force microscopy (AFM).

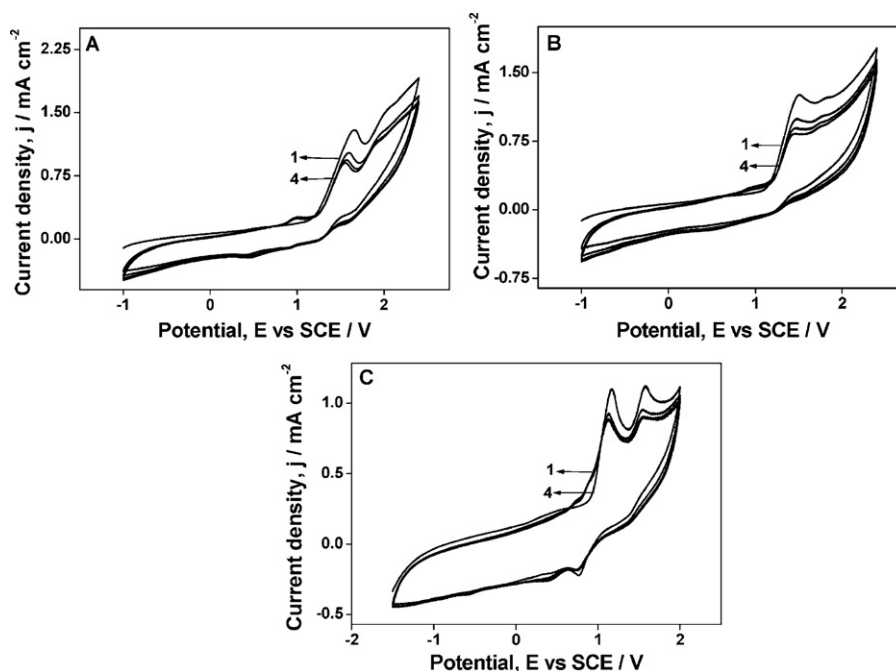


Fig. 3. Multisweep cyclic voltammograms (four cycles, 40 mV s^{-1}) of the GC electrode on the anodic oxidation of (A) 2,6-DMP, (B) 2,4-DMP and (C) 3,4-MDP in N_{2226} TFSI medium (concentrations of the phenols are 4 mM).

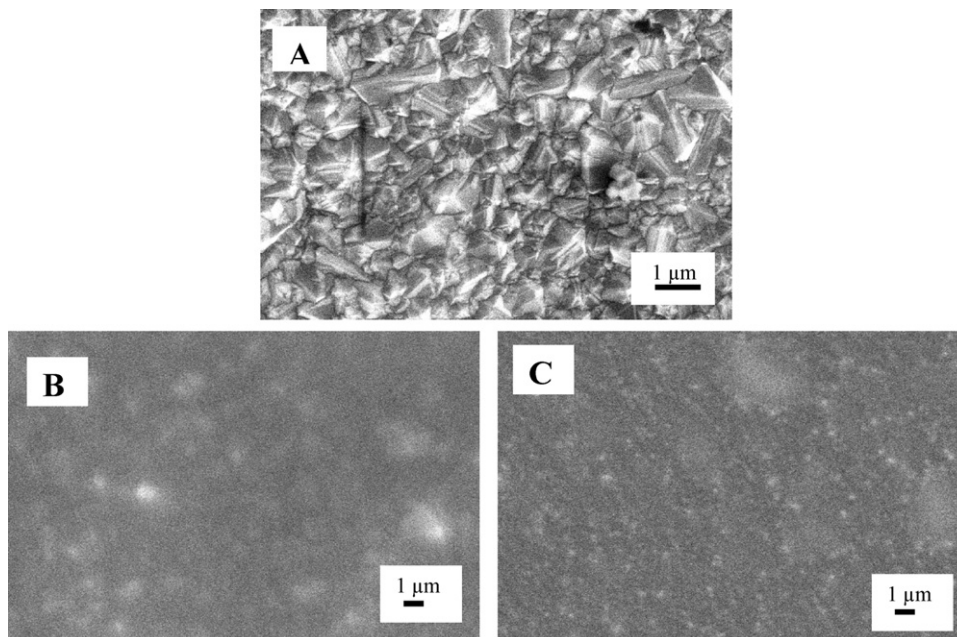


Fig. 4. SEM images of (A) unpolarised and polarised BDD electrode obtained by anodic polarisation (20 cycles) between 0.0 and 2.5 V in (B) neat EMIN and (C) EMIN containing 4 mM of 2,6-DMP. The magnification of (A) is 12.0 K and (B and C) is 1.0 K.

3.3. SEM analysis

As a typical example, the SEM images obtained by anodic cycling of the BDD between 0.0 and 2.5 V (20 cycles) in neat EMIN in presence and absence of 4 mM of the 2,6-DMP at a slow sweep rate of 40 mV s^{-1} are shown in Fig. 4B and C. For comparative study, the morphology of unpolarised BDD electrode is also shown in Fig. 4A. Fig. 4B reveals the formation of a thin organic layer masking the diamond crystals, due to the adsorption of the EMIN on the surface of diamond. Polarisation of the BDD in this medium containing 2,6-DMP reveals the deposition of thick organic polymers on the electrode surface (Fig. 4C). The SEM morphological analysis is

consistent with the very low I_{pa}^4/I_{pa}^1 value (0.29) obtained for 2,6-DMP in this medium (Table 2). The above analysis clearly suggests that RTIL itself gets adsorbed on the surface of the BDD electrode and this paves the way for severe deactivation of the electrode surface during the polarisation in presence of phenol.

3.4. AFM analysis

In Fig. 5A, AFM image (2-D and 3-D) of unpolarised BDD film (on silicon) is shown. The diamond film is continuous over the entire scanning area of the substrate with polycrystalline morphology containing well-faceted micro diamond crystallites of few μm in

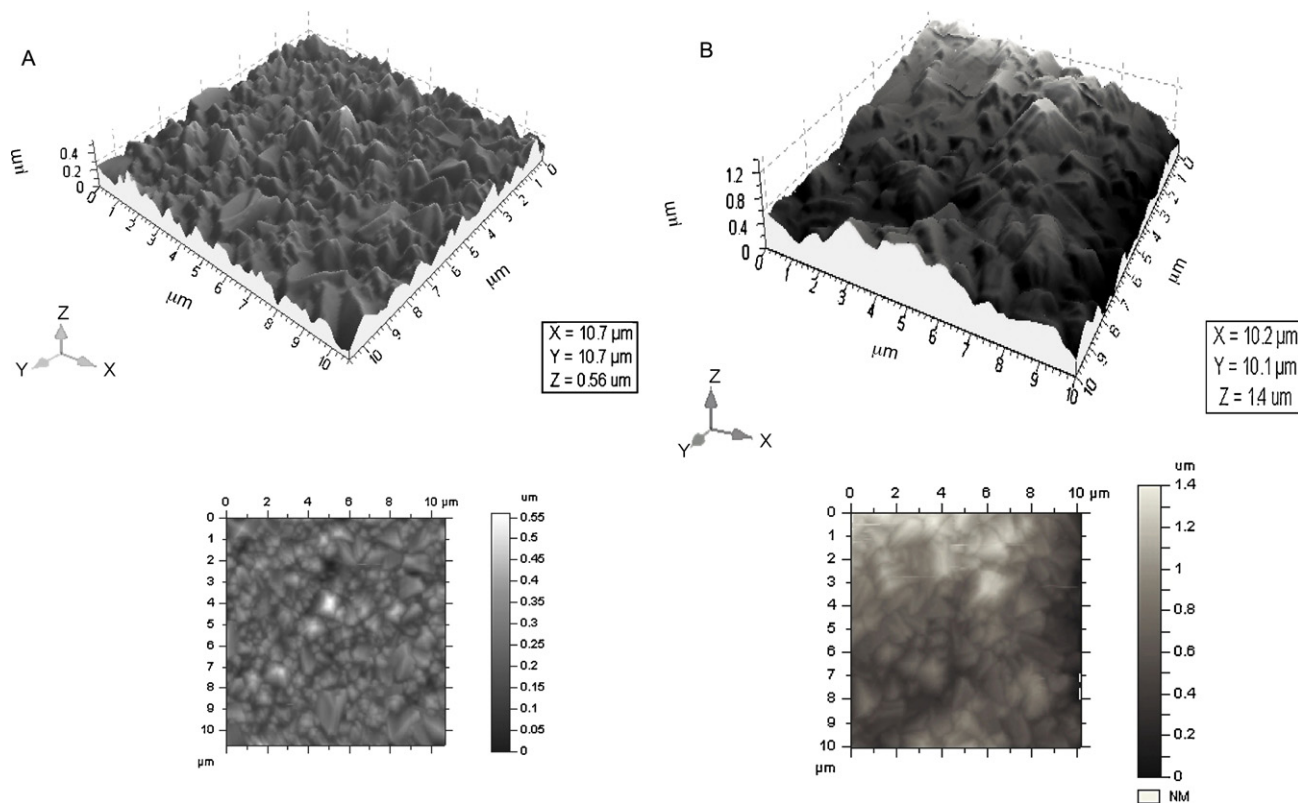


Fig. 5. AFM images of the BDD (A) unpolarised and (B) polarised in EMIN containing 4 mM of 2,6-DMP. The experimental conditions are the same as in Fig. 4.

diameter (Fig. 5A). Many twinned randomly oriented crystallites and grain boundaries are also clearly seen (Fig. 5A). Polarisation of the BDD in EMIN without 2,6-DMP conceals the distinct crystallites and facets to certain extent (figure not shown). The AFM picture of the BDD electrode (different location from Fig. 5A) obtained after anodic cycling between 0.0 and 2.5 V (20 cycles) in EMIN medium with 2,6-DMP at a slow sweep rate of 40 mV s^{-1} is shown in Fig. 5B. The morphological features completely change, where the deposited materials in between the boundaries and facets are clearly seen (Fig. 5B). Similar characteristic features are noted in the SEM and AFM pictures of the BDD obtained by polarisation in the other RTILs media containing 2,4-DMP and 3,4-MDP under the identical experimental conditions mentioned above.

3.5. CV studies in EMIN and TEMAMS media containing CH_3CN on the BDD

In order to understand the influence of solvent on the activation/deactivation behaviour of the BDD electrode, CH_3CN was added in small amounts (wt%) to the EMIN (curve a) and TEMAMS (curve b) media containing 2,6-DMP and the multisweep cyclic voltammograms were recorded at 40 mV s^{-1} for each addition in order to get the corresponding I_{pa}^4/I_{pa}^1 values. A plot of the I_{pa}^4/I_{pa}^1 values vs. the different weight percentages of CH_3CN added is shown in Fig. 6. With the addition of CH_3CN up to 50 wt%, an increase in I_{pa}^4/I_{pa}^1 values of 45% and 36% are noted in EMIN and TEMAMS media respectively. The above study shows that the presence of solvent in small amount can eliminate the electrode fouling only to certain extent.

The effect of addition of CH_3CN in large amount on the activation of the BDD during the anodic oxidation of 2,6-DMP in the above media was studied. Typical multisweep CVs of the BDD electrode in CH_3CN containing 0.1 M of TEMAMS and EMIN on the anodic oxidation of 2,6-DMP at 40 mV s^{-1} are shown in Fig. 7A

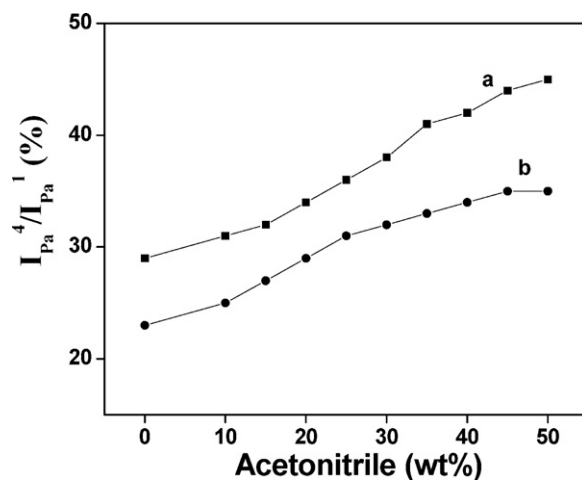


Fig. 6. Plot of the I_{pa}^4/I_{pa}^1 values (obtained from CV) of 2,6-DMP on the BDD in (a) EMIN (b) TEMAMS media vs. amount of CH_3CN (wt%) added.

and B respectively. From the figure, it is understandable that the oxidation potential of the 2,6-DMP increases from 1.5 V to 2.28 V in TEMAMS medium and 1.87 V to 2.24 V in EMIN medium. In a similar manner, a two-fold and three-fold increase in the peak current density is noted in TEMAMS and EMIN media and this may be associated with the decrease in the viscosity of the supporting electrolyte leading to an increase in the diffusion coefficient of the reactive species [24]. Further, the I_{pa}^4/I_{pa}^1 values increase sharply to an average value of 0.76 in both the RTILs on the BDD anode. Similar CV study carried out in N_{2226} TFSI medium containing 2,6-DMP shows good improvement in its corresponding I_{pa}^4/I_{pa}^1 value (0.74). From the above studies, it is noted that presence of solvent in excess can eliminate the electrode fouling to a greater extent

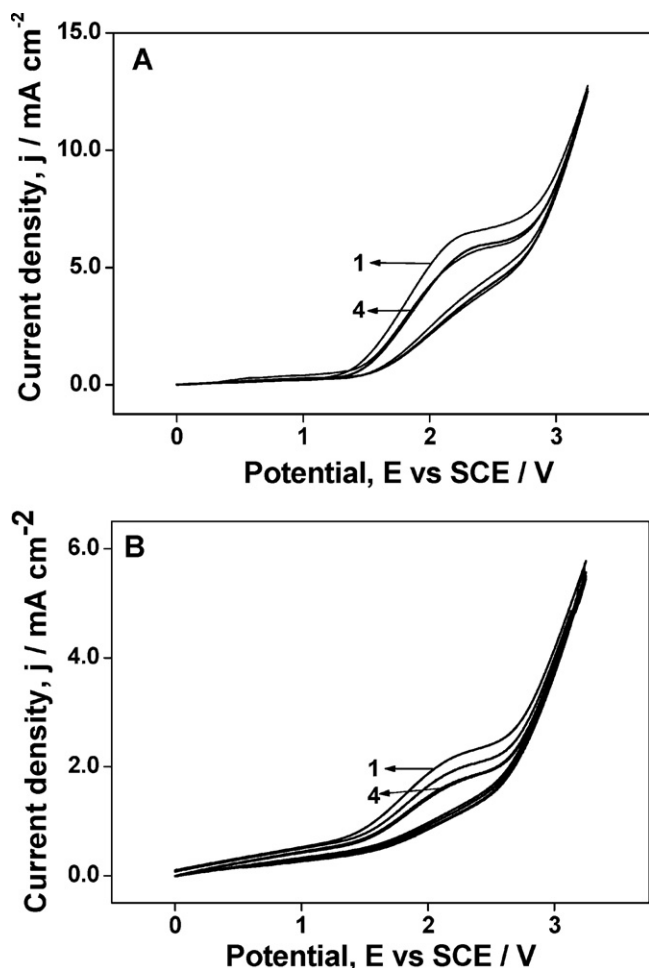


Fig. 7. Multisweep cyclic voltammograms (four cycles, 40 mV s⁻¹) on the anodic oxidation of 2,6-DMP on the BDD electrode in CH₃CN containing 0.1 M of (A) TEMAMS (B) EMIN media (concentration of the 2,6-DMP is 4 mM).

as this solvent provides reasonable solubility of organic reactants, intermediates and products.

Recent studies also support the addition of solvents to the RTILs media in activating the electrode surface during the preparative electrolysis of phenol compounds. For example, the yield of the main product, biphenol was found to improve in presence of excess of fluorinated solvents, to a large extent during the anodic coupling of 2,4-DMP in TEMAMS medium on the BDD anode. The formed products get dissolved easily in the fluorinated solvents and the deactivation of the BDD electrode is greatly suppressed [34].

It is well known that anodised BDD film contains sp³ functionalities such as alcoholic, ketonic and carboxylic groups in the carbon skeleton, which are hydrophilic in nature. The anodic polarisation of the BDD in the RTIL without phenol results in some specific interactions between the charged ionic species and sp³ functionalities, leading to the formation thin organic films on the facets of diamond crystals, as evidenced by SEM and AFM analysis. These van der Waals forces keep intact the polymeric products formed during the anodic polarisation of phenols resulting in the passivation of the electrode surface. Products formed during the oxidation of unsymmetrical phenolic compounds such as 3,4-MDP may try to come out of these weak forces and as a result of this, they show minimum fouling under identical experimental conditions. Addition of solvent such as CH₃CN in excess totally breaks these attractive forces and dissolves the products leading to complete activation of the electrode surface. No such organic films are formed on the unsaturated sp² functionalities (GC) and polycrystalline facets (Pt), as

noted from their SEM morphologies taken in these media without phenol (figures not shown). Further in-depth analysis must be necessary in order to investigate the composition and nature of the organic film formed on the BDD electrode surface.

The above voltammetric studies reveal that the investigated RTILs can be used as the media for oxidation of phenolic compounds only on the GC and Pt electrodes and in the case of the BDD electrode, highly polar solvents must be used along with the RTILs as these solvents provide high current density without any electrode passivation. Further studies are in progress to find out suitable ionic liquid media for the oxidation of phenols on the BDD anode without fouling.

4. Conclusions

The present voltammetric study reveals that the GC electrode shows wide anodic potential limit in all the RTILs followed by the BDD and Pt electrodes, wherein nonaflate based EMIN shows the highest anodic limit among the RTILs irrespective of the nature of electrodes employed. Multisweep voltammetric investigations suggest that the three phenolic compounds get oxidised at higher potential on the BDD electrode followed by Pt and GC and their oxidation potential in the three RTILs media increases in the order: TEMAMS < EMIN < N₂₂₂₆TFSI. Among the three phenolic compounds, 2,6-DMP shows highest oxidation potential followed by 2,4-DMP and 3,4-MDP in the three media. However, on the BDD electrode, a reverse trend on the anodic peak potential is noted. The above compounds show highest anodic peak current density on the GC electrode followed by the BDD and Pt in the three media. Particularly, in the TEMAMS medium, high anodic current density is noted. Further, the average I_{pa}^4/I_{pa}^1 values obtained for the three compounds are good on both the Pt and GC electrodes. However, on the BDD electrode, the I_{pa}^4/I_{pa}^1 values for 2,6-DMP and 2,4-DMP are found to be poor and in RTILs containing 3,4-MDP, it is somewhat better. The surface morphology of the fouled BDD electrode during the anodic polarisation in EMIN without and with 2,6-DMP had been characterised by SEM and AFM. The addition of CH₃CN in large amounts to this medium increases the activation of the BDD electrode surface.

Acknowledgements

The authors thank Director, CSIR-CECRI, Karaikudi for his keen encouragement in publishing this work. Financial support from DST, New Delhi (SR/S1/PC/62/2008) is greatly acknowledged.

References

- [1] US Environmental Protection Agency, Health and Environmental Effects Profile for Phenol, EPA/600/X-87/121.
- [2] F. Zimmermann, in: R. Taylor-Mayer (Ed.), Mutagenicity Testing in Environmental Pollution Control, Wiley, New York, 1985.
- [3] J. Grimm, D. Bessarabov, R. Sanderson, Desalination 115 (1998) 285.
- [4] G. Chen, Sep. Purif. Technol. 38 (2004) 11.
- [5] C. Nistor, J. Emne'us, L. Gorton, A. Ciucu, Anal. Chim. Acta 387 (1999) 309.
- [6] G. Marko-Verga, J. Emne'us, L. Gorton, T. Ruzgas, Trends Anal. Chem. 14 (1995) 319.
- [7] J. Wang, M. Jiang, F. Lu, J. Electroanal. Chem. 444 (1998) 127.
- [8] M. Gattrell, D.W. Kirk, Can. J. Chem. Eng. 68 (1990) 997.
- [9] X.Y. Li, Y.H. Cui, Y.J. Feng, Z.M. Xie, J.D. Gu, Water Res. 39 (2005) 1972.
- [10] P.I. Iotov, S.V. Kalcheva, J. Electroanal. Chem. 442 (1998) 19.
- [11] M. Gattrell, D.W. Kirk, J. Electrochem. Soc. 140 (1993) 903.
- [12] M. Gattrell, D.W. Kirk, J. Electrochem. Soc. 140 (1993) 1534.
- [13] J.L. Boudenne, O. Cercier, P. Bianco, J. Electrochem. Soc. 145 (1998) 2763.
- [14] N. Belhadj Tahar, A. Savall, Electrochim. Acta 54 (2009) 4809.
- [15] N. Belhadj Tahar, A. Savall, J. Appl. Electrochem. 39 (2009) 663.
- [16] P. Wasserschied, in: T. Welton (Ed.), Ionic Liquids in Synthesis, Wiley VCH Weinheim, Germany, 2003.
- [17] M. Armand, F. Endres, D.R. MacFarlane, H. Ohno, B. Scrosati, Nat. Mater. 8 (2009) 621.

- [18] D.R. MacFarlane, M. Forsyth, P.C. Howlett, J.M. Prinsle, J. Sun, G. Annat, W. Neil, E.I. Izgorodina, *Acc. Chem. Res.* 40 (2007) 1165.
- [19] H. Matsumota, in: H. Ohno (Ed.), *Electrochemical Aspects of Ionic Liquids*, Wiley, New Jersey, 2005.
- [20] P. Benhote, A.P. Dias, N. Papergeorgiou, K. Kalayasundaram, M. Gratzel, *Inorg. Chem.* 35 (1996) 1168.
- [21] J. Sun, M. Forsyth, D.R. MacFarlane, *J. Phys. Chem. B* 102 (1998) 8858.
- [22] C. Lagrost, D. Carrie, M. Vaultier, P. Hapiot, *J. Phys. Chem. A* 107 (2003) 745.
- [23] B.M. Quinn, Z. Ding, R. Moulton, A.J. Bard, *Langmuir* 18 (2002) 1734.
- [24] P. Hapiot, C. Lagrost, *Chem. Rev.* 108 (2008) 2238.
- [25] K. Sekiguchi, M. Atobe, T. Fuchigami, *J. Electroanal. Chem.* 557 (2003) 1.
- [26] H. Randriamahazaka, C. Plesse, D. Teyssie, C. Chevrot, *Electrochem. Commun.* 5 (2002) 77.
- [27] P. Damlin, C. Kvarnstrom, A. Ivaska, *J. Electroanal. Chem.* 570 (2004) 113.
- [28] A. Fujishima, Y. Einaga, T.N. Rao, D.A. Tryk (Eds.), *Diamond Electrochemistry*, Elsevier BKC, Tokyo, 2005.
- [29] M. Panizza, G. Cerisola, *Electrochim. Acta* 51 (2005) 191.
- [30] B. Marselli, J. Garcia-Gomez, P.A. Michaud, M.A. Rodrigo, C. Comninellis, *J. Electrochem. Soc.* 150 (2003) D79.
- [31] J. Iniesta, P.A. Michaud, M. Panizza, G. Cerisola, A. Aldaz, C. Comninellis, *Electrochim. Acta* 46 (2001) 3573.
- [32] J. Iniesta, P.A. Michaud, M. Panizza, C. Comninellis, *Electrochem. Commun.* 3 (2001) 346.
- [33] I.M. Malkowsky, U. Griesbach, H. Putter, S.R. Waldvogel, *Eur. J. Org. Chem.* (2006) 4569.
- [34] A. Kirste, M. Nieger, I.M. Malkowsky, F. Stecker, A. Fischer, S.R. Waldvogel, *Chem. Eur. J.* 15 (2009) 2273.
- [35] A. Kirste, G. Schnakenburg, F. Stecker, A. Fischer, S.R. Waldvogel, *Angew. Chem. Int. Ed.* 49 (2010) 971.
- [36] J. Sun, D.R. MacFarlane, M. Forsyth, *Ionics* 3 (1997) 356.
- [37] A. Manivel, D. Velayutham, M. Noel, *J. Electroanal. Chem.* 655 (2011) 79.
- [38] F. Loyson, C. Imrie, S. Gouws, B. Barton, E. Kruger, *J. Appl. Electrochem.* 39 (2009) 1087.
- [39] M. Narmadha, M. Noel, V. Suryanarayanan, *J. Electroanal. Chem.* 655 (2011) 103.
- [40] V. Suryanarayanan, M. Noel, *J. Electroanal. Chem.* 642 (2010) 69.
- [41] F. Wantz, C.E. Banks, R.G. Compton, *Electroanalysis* 17 (2005) 1529.
- [42] E.R. Lowe, C.E. Banks, R.G. Compton, *Electroanalysis* 17 (2005) 1627.
- [43] E.R. Lowe, C.E. Banks, R.G. Compton, *Anal. Bioanal. Chem.* 382 (2005) 1169.